Syntheses, crystal structures and magnetic properties of three novel cobalt(II) complexes containing imidazole derivative groups†

Hong Yang,[a] Jia-Min Chen,[a] Jing-Jia Sun,[a] Shi-Ping Yang,*[a] Jie Yu,[b] Hong Tan[b] and Wei Li*[b]

Received 19th May 2008, Accepted 23rd January 2009
First published as an Advance Article on the web 23rd February 2009
DOI: 10.1039/b808385a

Three Co(II) complexes with the formulas: $\{[Co_2(Bib)_3Cl_2]Cl(CH_3COO)\}\cdot CH_3OH\cdot H_2O$ (**1**), $[Co_2(Bib)_3Cl_2]Cl_2\cdot(CH_3OH)_2\cdot H_2O$, (**2**) and $[Co_3K_1(Tib)_2(CH_3COO)_6]PF_6$ (**3**), were obtained by self-assembly of a cobalt(II) salt with Bib and Tib (Bib = 1,3-bis(4,5-dihydro-1*H*-imidazol-2-yl)-benzene; Tib = 1,3,5-tris(4,5-dihydro-1*H*-imidazol-2-yl)benzene) and were structurally and magnetically characterized. X-Ray single-crystal diffraction showed that each Co(II) ion was in a highly distorted tetrahedral coordination geometry with a *cis–trans* ratio of 1 : 2 from the Bib ligand, which functioned in a bidentate fashion in the binuclear triple-helical $[Co_2(Bib)_3Cl_2]^{2+}$ cations in **1** and **2**. In the $[Co_3K_1(Tib)_2(CH_3COO)_6]^-$ anions in **3**, each Co(II) ion was also in a highly distorted tetrahedral coordination geometry and the Tib ligands acted in an offset fashion in C, C, C and A, A, A coordination to the Co(II) ions with π–π stacking interactions between two benzene rings from the Tib ligand in the cluster cation. Each Tib ligand in a cluster unit acted as a tridentate entity to coordinate three Co(II) ions resulting in a cylinder-like cluster structure. The intermolecular hydrogen bonds in the solid-state resulted in the well-shaped 2D layer network which formed a honeycomb in **1**, the 3D supramolecular architecture which was connected to the 2D sheet into 3D in **2** and the 3D supramolecular architecture, which was extended into a well-shaped 2D honeycomb layer network in **3**. The results from magnetic data, in the high-temperature region, showed that **1** and **2** obeyed the Curie–Weiss law with a Weiss constants $\theta = -12.3$, and −9.8 K and a Curie constants $C = 5.31$ and 5.32 cm^3 K $mo1^{-1}$, respectively, indicating antiferromagnetic interactions between adjacent cobalt(II) ions. Both complex **1** and **2** showed magnetic ordering at low temperature due to the canting effect. The zero-field AC magnetic susceptibility measurements for **1** and **2** displayed a maximum which was frequency dependent owing to a slow relaxation process, which could be caused by either domain wall movements or spin-glass behaviours.

Introduction

Since the mid-1990s, research in coordination chemistry has been strongly influenced by the development of metallo-supramolecular chemistry,[1] which involves the design and preparation of intricate polymetallic coordination aggregates with specific structures or functions.[2] The creation of supramolecular networks can be accomplished by the judicious combinations of organic ligands and metals, thus exploiting the ability of metal–ligand coordination bonds to provide simple and controlled routes to 1D, 2D, or 3D metal–organic frameworks (MOFs),[3] which constitute an exotic class of coordination polymers and may exhibit unique properties, including adsorption, magnetism, and others.[4–9] The bottom-up assembly of MOFs from metal ions and organic linkers is one of the cornerstones of crystal engineering. In this context, the final architecture might exhibit additional levels of supramolecular organization, by exploiting other weak interactions such as hydrogen bonding or π–π interactions, among others. We have been interested in the preparation of novel MOFs with relevance to the area of molecular magnetism. One of our goals is to organize magnetic coordinated complexes with predetermined structures in order to gain control of the magnetic properties of the final material.

For some time, we have been exploring the coordination chemistry of imidazole-based ligands as the product of the attempted synthesis of transition metal complexes as structural models of some metalloenzymes and crystal engineering.[10,11] We have now turned our attention to the ligand-containing imidazole derivative groups (Bib = 1,3-bis(4,5-dihydro-1*H*-imidazol-2-yl)-benzene; Tib = 1,3,5-tris(4,5-dihydro-1*H*-imidazol-2-yl)benzene, Scheme 1) as a polydentate coordination mode. These ligands have been previously employed in the preparation of very interesting MOFs aimed at fulfilling various roles such as host–guest functions.[12–13] The reactivity of Bib and Tib with simple complexes of cobalt(II), was explored here in order to construct extended magnetic materials. Fortunately, three new novel coordinated compounds $\{[Co_2(Bib)_3Cl_2]Cl(CH_3COO)\}\cdot CH_3OH\cdot H_2O$ (**1**), $[Co_2(Bib)_3Cl_2]Cl_2\cdot(CH_3OH)_2\cdot H_2O$, (**2**) and $[Co_3K_1(Tib)_2(CH_3COO)_6]PF_6$ (**3**), can be obtained by the vapour diffusion method.

[a]*Department of Chemistry, College of Life and Environmental Science, Shanghai Normal University, Shanghai, 200234, P. R. China. E-mail: shipingy@shnu.edu.cn*
[b]*National Engineering Research Center for Compounding and Modification of Polymeric Materials, Guiyang, Guizhou 550014, P. R. China. E-mail: dearweili@gmail.com*

† Electronic supplementary information (ESI) available: Additional structural diagrams. CCDC reference numbers 667565, 667566 and 667567 for **1**, **2** and **3**, respectively. For ESI and crystallographic data in CIF or other electronic format see DOI: 10.1039/b808385a

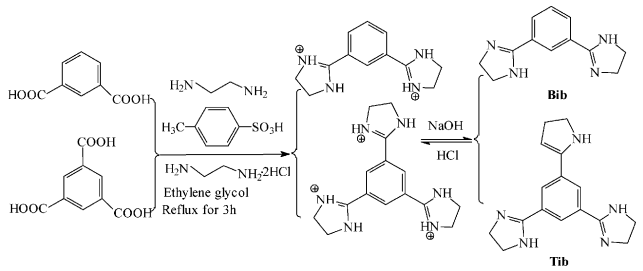

Scheme 1 Synthesis of Bib and Tib.

Therefore in this paper, we reported the preparation and characterization of these compounds by elemental analyses (EA), infrared spectra (IR), thermogravimetry (TG) and X-ray single-crystal diffraction. The magnetic properties of the complexes were also investigated.

Experimental

All reagents are commercially available and used as received. Solvents are dried by conventional procedures prior to use. All samples are thoroughly dried prior to elemental analyses.

Physical measurements

The C, H and N elemental analyses were performed on a Perkin-Elmer 204 elemental analyser. The IR spectra were recorded on a Nicolet Avatar 370 DTGS spectrophotometer with KBr discs in the 4000–400 cm^{-1} regions. The ^1H NMR spectra were performed on a Varian 300 MHz spectrometer with TMS as reference, using D_2O or CD_3OD as matrix. The UV–vis spectrophotometric investigations in the solvent and solid-state were performed on a UV-2450 spectrophotometer (Shimadzu instruments) in a range from 180–800 nm. Melting points were determined on a XT4A microscope and were uncorrected. The TGA were performed under N_2 atmosphere on a Shimadzu DTG-60H instrument at a temperature ramp rate of 10 °C min^{-1}. Magnetic susceptibility was measured with a Quantum Design SQUID MPMS XL-7 magnetometer for **1** and **2**. The measurements are taken from 2–300 K. Selected samples are contained in a gel capsule sample holder. The magnetic susceptibility is corrected for the gel capsule and core diamagnetism with Pascal's constants.[14] Magnetic susceptibility is measured with a Quantum Design SQUID PPMS-9 magnetometer for **3**.

Preparation of ligands and metal complexes

Synthesis of Bib[13]. 1,3-Benzenedicarboxylic acid (2.31 g, 13.9 mmol), ethylenediamine (3.70 cm^3, 50 mmol), ethylenediamine dihydrochloride (6.64 g, 50 mmol) and toluene-*p*-sulfonic acid (0.208 g, 1.09 mmol) were added to the solvent of ethylene glycol (20 cm^3), and the mixture solution was refluxed for 3 h. About half of the ethylene glycol solvent was then slowly removed by distillation. The residue was dissolved in a mixture of water (40 cm^3) and concentrated HCl (11 M, 3 cm^3). The addition of 50% aqueous NaOH gave a yellow precipitate that was purified by recrystallization. The ligand Bib was obtained in *ca.* 80% yield based on 1,3-benzenedicarboxylic acid (*ca.* 2.38 g). M.p. > 250 °C. Anal. calcd for $C_{12}H_{14}N_4$: C 67.27, H 6.59, N 26.15. Found: C 67.15, H 6.61, N 26.10%. ^1H NMR (300 MHz, D_2O):δ 3.60 (b, 4H, NH–CH_2), 4.70 (b, 4H, N–CH_2), 7.40 (t, 1H, C_6H_4), 7.70 (d, 2H, C_6H_4), 7.90 (s, 1H, C_6H_4). Main IR bands (KBr, cm^{-1}): 3158 m, 2936 m, 2862 m, 1620 s, 1568 s, 1495 s, 1306 m, 1270 s, 1191 w, 1085 w, 980 m, 907 w, 808 w, 699 m, 652 w, 531 w, 486 w.

Synthesis of Tib. 1,3,5-Benzenedicarboxylic acid (1.51 g, 7.18 mmol), ethylenediamine (1.58 cm^3, 23.7 mmol), ethylenediamine dihydrochloride (3.15 g, 23.7 mmol) and toluene-*p*-sulfonic acid (0.216 g, 1.12 mmol) were added to the solvent ethylene glycol (10 cm^3), and the mixture solution was refluxed for 5 h. About half of the ethylene glycol solvent was then slowly removed by distillation. The residue was dissolved in a mixture of water (40 cm^3) and concentrated HCl (11 M, 3 cm^3). The addition of 50% aqueous NaOH gave a yellow precipitate that was purified by recrystallization. The ligand Tib was obtained in *ca.* 30% based on 1,3,5-benzenedicarboxylic acid (*ca.* 620 mg). M.p. > 250 °C. Anal. calcd for $C_{15}H_{18}N_6$: C 63.81, H 6.43, N 29.77. Found: C 63.78, H 6.49, N 29.80%. ^1H NMR (300 MHz, CD_3OD): δ 8.24 (s, 3H, C_6H_3), 3.31 (t, 12H, CH_2). Main IR bands (KBr, cm^{-1}): 3743 w, 3423 (s, b), 3268 (m, b), 3135 s, 2934 m, 2869 m, 1624 s, 1572 s, 1500 s, 1329 w, 1280 s, 1185 w, 1039 w, 985 w, 698 m, 526 (m, b).

Synthesis of $\{[Co_2(Bib)_3Cl_2]Cl(CH_3COO)\}\cdot CH_3OH\cdot H_2O$, 1. A solution of $Co(CH_3COO)_2\cdot 4H_2O$ (0.249 g, 1.0 mmol) in methanol (15 mL) was slowly added to a methanolic solution (10 mL) of Bib (0.214 g, 1.0 mmol), and the pH value was adjusted to *ca.* 7.5. by hydrochloric acid. The mixture was stirred for 30 min. After three days, the blue-purple crystalline solid of **1** was obtained by vapour diffusion of diethyl ether (*ca.* 75% yield based on Bib. Calcd for $C_{39}H_{51}Cl_3Co_2N_{12}O_4$: C 47.99, H 5.27, N 12.77. Found: C 47.88, H 5.26, N 12.75%). Main IR bands (KBr, ν, cm^{-1}): 3235 m, 2879 w, 1729 s, 1602 m, 1569 m, 1514 s, 1466 m, 1342 w, 1278 s, 1020 m, 787 s, 798 m, 560 w, 435 w.

Synthesis of $[Co_2(Bib)_3Cl_2]Cl_2\cdot(CH_3OH)_2\cdot H_2O$, 2. A solution of $CoCl_2\cdot 6H_2O$ (0.238 g, 1.0 mmol) in methanol (10 mL) was slowly added to a methanolic solution (10 mL) of Bib (0.214 g, 1.0 mmol). The mixture was stirred for 30 min. After seven days, the blue-purple block crystalline solid of **2** was obtained by vapour diffusion of diethyl ether (*ca.* 65% yield based on Bib. Calcd for $Co_2C_{38}H_{52}N_{12}O_3Cl_4$: C 46.36, H 5.32, N 17.07. Found: C 46.30, H 5.18, N 17.01%). Main IR bands (KBr, ν, cm^{-1}): 3341 m, 3238 m, 2881 w, 1617 m, 1572 m, 1510 s, 1460 m, 1339 w, 1282 s, 1016 m, 791 s, 700 m, 567 w, 436 w.

Synthesis of $[Co_3K_1(Tib)_2(CH_3COO)_6]PF_6$ 3. A solution of $Co(CH_3COO)_2\cdot 4H_2O$ (0.249 g, 1.0 mmol) in methanol (10 mL) was slowly added to a methanolic solution (10 mL) of Tib (0.262 g, 1.0 mmol). Then a solution of KPF_6 (0.184 g, 1 mmol) in methanol (5 mL) was poured in the mixture. Lastly, the mixture was stirred for 30 min. After a month, the blue-purple block crystalline solid of **3** was obtained by vapour diffusion of diethyl ether (*ca.* 45% yield based on Tib. Calcd for $Co_3C_{42}H_{54}N_{12}O_{12}KPF_6$: C 39.42, H 4.25, N 13.13. Found: C 39.15, H 4.29, N 13.59%). Main IR bands (KBr, ν, cm^{-1}): 3436 (m, b), 3072 w, 2946 w, 2876 w, 1613 s, 1580 s, 1515 s, 1474 m, 1397 s, 1335 m, 1283 m, 1188 w, 846 s, 673 m.

Table 1 The crystallographic data for complexes **1**, **2** and **3**

	1	**2**	**3**
Empirical formula	$C_{39}H_{51}Cl_3Co_2N_{12}O_4$[a]	$C_{38}H_{52}Cl_4Co_2N_{12}O_3$[b]	$C_{42}H_{54}Co_3F_6KN_{12}O_{12}P$
Formula weight	976.13[a]	984.58[b]	1279.83
T/K	298(2)	298(2)	298(2)
λ/Å	0.71073	0.71073	0.71073
Crystal system	Monoclinic	Triclinic	Hexagonal
Space group	$C2/c$	$P\bar{1}$	$P6_322$
a/Å	25.458(2)	10.976(1)	14.575(3)
b/Å	13.8919(9)	14.375(2)	14.575(3)
c/Å	27.979(2)	14.749(2)	13.889(4)
α/°	90	78.341(2)	90
β/°	110.223(1)	88.920(2)	90
γ/°	90	74.691(2)	120
V/Å^3	9285(1)	2197.0(4)	2555(1)
Z	8	2	2
ρ_c/g cm^{-3}	1.397	1.485	1.664
μ/mm^{-1}	0.939	1.050	1.169
F(000)	3994.3	1016	1309.3
Crystal size/mm	0.518 × 0.506 × 0.325	0.477 × 0.176 ×0.180	0.401 × 0.067 × 0.031
θ range/°	1.70–27.00	1.84–25.50	1.61–26.99
Limiting indices (h, k, l)	$-30 < h < 21$, $-15 < k < 16$, $-33 < l < 33$	$-13 < h < 10$, $-17 < k < 17$, $-15 < l < 17$	$-13 < h < 18$, $-18 < k < 17$, $-17 < l < 17$
Reflections collected/unique	8149/5676	11 570/8185	12 712/1515
R_{int}	0.0640	0.0712	0.1521
Refinement method	Full-matrix least-squares on F^2	Full-matrix least-squares on F^2	Full-matrix least-squares on F^2
Data/restraints/parameters	8149/123/589	8060/0/536	1515/6/133
Goodness of fit on F^2	1.001	0.997	1.000
R_1, wR_2 (obs)	0.0588, 0.1826	0.0664, 0.1740	0.1205, 0.1583
R_1, wR_2 (all)	0.0767, 0.1895	0.0974, 0.1964	0.1205, 0.1748
Largest and hole/e Å^{-3})	1.099 and –0.367	1.753 and –0.924	0.362 and –0.434

[a] Containing the six hydrogen atoms of a methanol and a water molecules that were not found. [b] Containing the two hydrogen atoms of a water molecule that were not found.

X-Ray crystallography

Diffraction intensities for **1**, **2** and **3** are collected (hemisphere technique) on a Bruker SMART Platform CCD diffractometer at 298 K with a molybdenum tube ($\lambda_{K\alpha}$ = 0.71073 Å), and the absorption correction is applied with the SADABS program.[15] The structure solution and full-matrix least-squares refinement based on F^2 are performed with the SHELXS-97 and SHELXL-97[16] program packages, respectively. All the non-hydrogen atoms are refined anisotropically. Hydrogen atoms of the organic ligands are generated geometrically (C–H 0.95 or 0.99 Å for **1**, and **2**, 0.98 or 0.99 for **3**, O–H 0.84 Å for **2** and N–H 0.88 Å). Analytical expressions of neutral-atom scattering factors are employed, and anomalous dispersion correction incorporated.[17] Both complex **1** and **3** are solved by restrained refinement and constrained refinement because of disordered solvents or anions. For the complex **1**, the Cl3 atom is disorder over two sites (Cl3 and Cl3′) and the site occupancy of the major components is 0.80. The oxygen atom from the solvent water molecule is also disordered over two sites O1w and O2w with the occupancy factor being 0.80 and 0.20. In addition, the methanol molecule is disordered over two positions (0.75 : .25). The H positions of the methanol and water molecules of compound **1** and of the water molecule of compound **2** were not determined. The PF_6^- anions from the complex **3**, the P and F atoms are all in special position and the occupancy factors for P, F1, F2 and F3 atoms were all 0.1667, 0.3333, 0.3333 and 0.3333, respectively. The crystallographic data for the three complexes are summarized in Table 1. Selected bond distances and angles are given in Table 2.

Results and discussion

Synthesis

The reaction of diamine and dicarboxylic acid and tricarboxylic acid depends very much on the reaction conditions, such as the ratio of the reactants, solvent, concentration and temperature.[13] The reaction of 1,3-benzenedicarboxylic acid and 1,3,5-benzenetricarboxylic acid with 1,2-diaminoethane in the presence of acid catalysis (toluene-*p*-sulfonic acid) offered Bib in 80% and Tib in 30% yield based on 1,3-benzenedicarboxylic acid and 1,3,5-benzenetricarboxylic acid under reflux in ethylene glycol solution for 3 h, respectively, as shown in Scheme 1. EA, NMR and IR spectra confirmed the target product. The cobalt(II) complexes with the formulas: $\{[Co_2(Bib)_3Cl_2]Cl(CH_3COO)\}\cdot CH_3OH\cdot H_2O$, (**1**), $[Co_2(Bib)_3Cl_2]Cl_2\cdot(CH_3OH)_2\cdot H_2O$, (**2**) and $[Co_3K_1(Tib)_2(CH_3COO)_6]PF_6$ (**3**), were obtained by the vapour diffusion method due to the reaction of cobalt acetate tetrahydrate and cobalt chloride hexhydrate with Bib and Tib ligands, respectively, and were characterized by EA, NMR and IR methods. Although there were four possible coordination configurations, A,C-*cis*, C,A-*cis*, A,A-*trans* and C,C-*trans* for Bib, and four modes C,C,C; C,C,A; A,A,A and A,A,C for Tib, as shown in Scheme 2, the

Table 2 Selected bond distances (Å) and angles (°) for complexes **1**, **2** and **3**

1			
Co(1)–N(1)	2.000(4)	Co(1)–N(9)	2.020(4)
Co(1)–N(5)	2.007(3)	Co(1)–Cl(1)	2.261(1)
Co(2)–N(3)	2.002(4)	Co(2)–N(7)	2.020(4)
Co(2)–N(11)	2.012(4)	Co(2)–Cl(2)	2.256(1)
Co(1)–Co(2)	5.478 (4)		
N(1)–Co(1)–N(5)	109.7(2)	N(9)–Co(1)–Cl(1)	103.0(1)
N(1)–Co(1)–N(9)	120.4(2)	N(1)–Co(1)–Cl(1)	104.4(1)
N(5)–Co(1)–N(9)	112.6(2)	N(5)–Co(1)–Cl(1)	105.0(1)
N(3)–Co(2)–N(11)	117.0(2)	N(3)–Co(2)–Cl(2)	102.7(1)
N(11)–Co(2)–N(7)	109.2(2)	N(11)–Co(2)–Cl(2)	106.5(1)
N(3)–Co(2)–N(7)	115.8(1)	N(7)–Co(2)–Cl(2)	104.1(1)
2			
Co(1)–N(11)	1.998(4)	Co(2)–N(9)	2.007(4)
Co(1)–N(7)	2.018(4)	Co(2)–N(3)	2.021(4)
Co(1)–N(1)	2.023(5)	Co(2)–N(5)	2.022(4)
Co(1)–Cl(1)	2.264(2)	Co(2)–Cl(2)	2.259(2)
Co(1)–Co(2)	5.584 (2)		
N(11)–Co(1)–N(7)	110.5(2)	N(9)–Co(2)–N(3)	118.9(2)
N(11)–Co(1)–N(1)	115.4(2)	N(9)–Co(2)–N(5)	106.3(2)
N(7)–Co(1)–N(1)	113.2(2)	N(3)–Co(2)–N(5)	114.1(2)
N(11)–Co(1)–Cl(1)	108.8(1)	N(9)–Co(2)–Cl(2)	103.9(1)
N(7)–Co(1)–Cl(1)	103.9(1)	N(3)–Co(2)–Cl(2)	102.8(1)
N(1)–Co(1)–Cl(1)	104.0(1)	N(5)–Co(2)–Cl(2)	110.1(1)
3			
Co–O(1)	1.991(9)	Co–N(1)	2.026(5)
O(1a)–Co–O(1)	79.8(6)	O(1)–Co–N(1a)	109.9(3)
O(1)–Co–N(1)	111.3(3)	N(1a)–Co–N(1)	125.5(3)

Symmetry code for **3**: (a) x, $x - y + 1$, $-z + 1/2$.

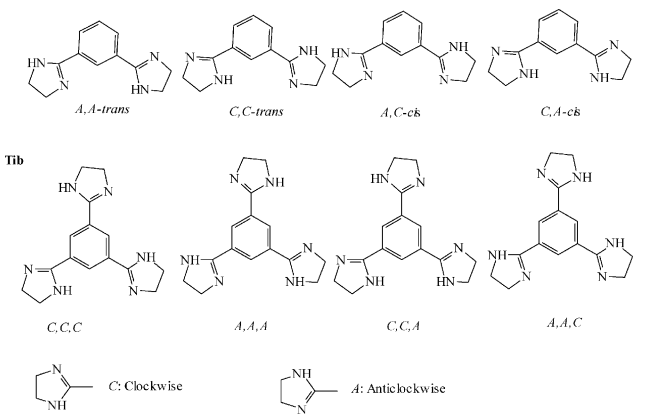

Scheme 2 Possible coordination configurations of Bib and Tib.

three coordination forms C,A-*cis*, A,A-*trans* and C,C-*trans* were all found in **1** and **2** for Bib, and the two donated modes C,C,C and A,A,A were also found in **3** for Tib. In our work, we tried to complete more tests using different counter anions to examine their effect. Unfortunately, we did not obtain the other counter anion single-crystal compound.

Physical and spectroscopic study

EA satisfactorily indicated that the complex contained a unit which was composed of Bib ligands, and cobalt metal ions with a molar ratio of 3 : 2 in **1** and **2**. However, the data from **3** confirmed that the molar ratio of Tib ligand and cobalt metal ions was 2 : 3. These results were in agreement with the crystal structure results of **1**, **2** and **3** in the solid-state.

The IR spectra showed a few peaks at *ca.* 3158, 2936 and 1620 cm^{-1} for Bib and 3135, 2934 and 1624 cm^{-1} for Tib, which were assigned to the stretching vibration of the C–H groups of the benzene ring, C–H from CH_2 groups of the hydrogenated imidazole ring and C=N groups of the hydrogen imidazole ring, respectively. It should be noted that there was a red-shift of the C=N groups stretching vibration from 1620, 1620 and 1624 to 1602, 1617 and 1613 cm^{-1} in comparison with those for **1**, **2** and **3**, respectively, indicating direct coordination of the nitrogen atoms in C=N groups.

The data from the electronic spectra of the ligands Bib and Tib and the complexes **1**, **2** and **3** exhibited intense absorption bands at *ca.* 260 and 310 nm in methanol, 210 and 280 nm in the solid-state, respectively, which can be attributed to $\pi \rightarrow \pi^*$ transition of the conjugated benzene and hydrogenated imidazole chromospheres. In the visible region, complexes **1**, **2** and **3** exhibited a strong band at *ca.* 620, 620 and 605 nm in the solid-state, respectively, which were assigned to the d–d ($^4A_2 \rightarrow {}^4T_2$) transition.

Thermogravimetric analyses

The thermogravimetric analysis curve of **1** confirms that the process of decomposition of the complex has two stages. The first stage decomposition was in the range of 70–160 °C and the weight loss was about 5.6%, indicating the evaporation of water and methanol molecules (calcd 5.1%). The DTA curve also showed a weak endothermic peak. The second weight loss occurs in the range of 324–698 °C and is characteristic of the decomposition of the organic moiety. A weak endothermic peak and a strong exothermic peak appeared on the DTA curves, which were attributed to evaporation of the solvent and organic molecule combustion, respectively.

The thermogravimetric analysis curve of **2** was slightly different from that of **1**. The first stage decomposition was in the range of 70–120 °C and the weight loss was about 3.2%, indicating the evaporation of crystal water (calcd 3.7%). The DTA curve also showed a weak endothermic peak. The second stage decomposition was in the range of 120–303 °C. The weight loss was about 6.7%, which corresponded to the loss of methanol molecules (calcd 6.5%). A weak endothermic peak also appeared on the DTA curve and was attributed to evaporation of methanol molecules. The last stage decomposition was from 303–676 °C. The weight loss was about 64.1%, suggesting loss of the ligand (calcd 63.6%), and indicated that the residue was $CoCl_2$. A weak exothermic and a strong endothermic peak around 560 and 630 °C, respectively, on the DTA curve, which were attributed to organic molecule combustion.

The thermogravimetric analysis curve of **3** was different from those of **1** and **2**. A two-step weight loss (24.8%) between 310 and 340 °C and a gradual loss of 45.0% among from 340–600 °C could be observed. The observed total weight loss corresponds to the removal of the organic (C, H and N) part which accounts for 66.2% of the mass of **3**. These results indicated that the residue was the mixture of Co_2O_3 and KPF_6. A weak exothermic and a strong endothermic peak appeared around 450 and 570 °C,

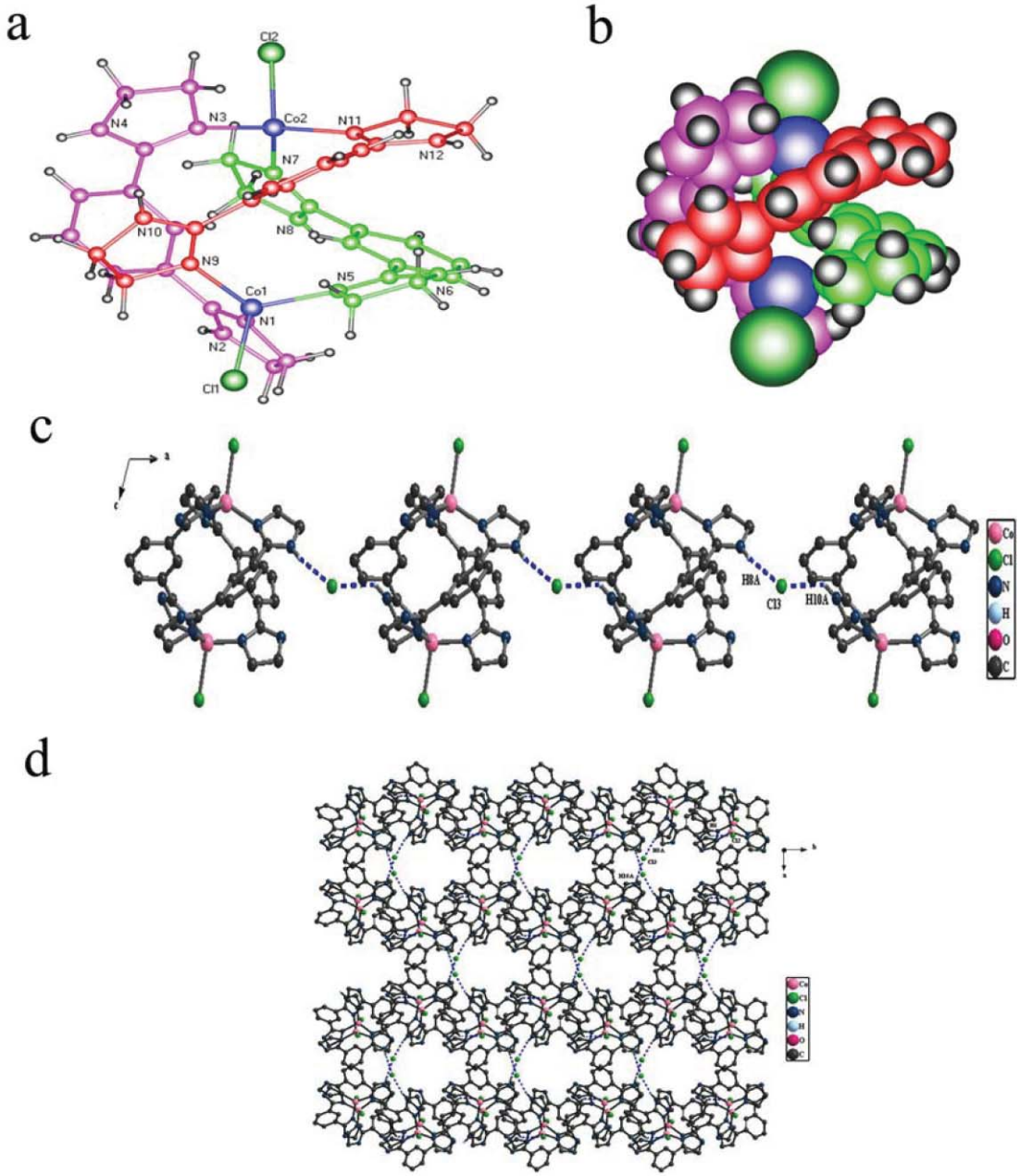

Fig. 1 (a) Perspective view of the binuclear cation in **1**. (b) Space-filling representation of the triple helical structure (c) 1D the chain (d) 2D structure.

respectively, on the DTA curve and were attributed to organic molecule decomposition.

Crystal structures

{[Co_2(Bib)$_3Cl_2$]Cl(CH_3COO)}·CH_3OH·H_2O, 1. The complex of **1** crystallized in the space group *C*2/*c*, and the asymmetric unit contained 8 complex molecules. X-Ray single-crystal diffraction showed that the crystal structure of **1** consisted of discrete binuclear $[Co_2(Bib)_3Cl_2]^{2+}$ cations, an acetate anion, a methanol and a water molecule. The binuclear $[Co_2(Bib)_3Cl_2]^{2+}$ cation is shown in Fig. 1, and shows that the cation is a triple-helical fashion. Each Co(II) ion was coordinated to nitrogen atoms from three different ligands and a chloride anion, resulting in a highly distorted tetrahedral coordination geometry. The coordination angles around the Co(1) and Co(2) ions were in the range of 103.0(1)–120.4(2)° and 102.7(1)–117.0(2)°, respectively. In the binuclear cation, the Co–N and Co–Cl bond lengths were in the range of 2.000(4)–2.020(4) Å and 2.256(1)–2.261(1) Å, respectively, in which the Co–Cl bond length was longer than that of the Co–N bond. The Co···Co separation in the cation was 5.478(4) Å. It is worth noting that the Bib ligands acted in two ways in *cis* (C,A), and *trans* (A,A and C,C) coordination to the Co(II) ions with a *cis–trans* ratio of 1 : 2, as shown in Fig. 1a and Scheme 2. These results are different from that of silver(I) complexes[12], in which the Bib ligand is only found in the *cis* coordination configuration. Three benzene rings from the Bib ligand in the binuclear cation were interlaced with each other

Table 3 Hydrogen bond parameters for **1**, **2** and **3**

C(N)–H···Cl	*d*(C(N)–H)/Å	*d*(H···Cl(O))/Å	*d*(C(N)···Cl(O))/Å	∠C(N)HCl(O)/°
1				
N4–H(4)···O(1 W)	0.88	1.98(2)	2.813(6)	158
N6–H(6A)···O2^{ii}	0.88	2.05(2)	2.841(6)	150
N12–H(12C)···O1^{ii}	0.86	2.06(2)	2.879(6)	156
N(8)–H(8A)···Cl(3)	0.88	2.40(1)	3.258(5)	164
N(10)–H(10A)···Cl(3)^{iii}	0.88	2.55(1)	3.279(5)	141
C(6)–H(6)···Cl(2)^{i}	0.95	2.77(1)	3.554(5)	140
2				
N2–H2···O2^{i}	0.88	2.31(1)	2.942(9)	129
N4–H4···O3^{ii}	0.88	1.97(2)	2.842(8)	172
N6–H6···O1^{i}	0.86	2.02(2)	2.756(9)	141
O2–H2D···Cl4	0.84	2.56(1)	3.304(8)	148
O3–H3···Cl3	0.84	2.70(2)	3.077(6)	109
N8–H8A···Cl3	0.88	2.48(1)	3.1995(5)	140
N10–H10···Cl3	0.88	2.67(1)	3.226(5)	123
N12–H12···Cl4	0.88	2.35(2)	3.220(6)	169
3				
N2–H2C···O2^{i}	0.88	2.38(1)	3.02(2)	130
C5–H5A···O2^{ii}	0.95	2.25(1)	3.17(2)	166
C2–H2B···F3^{iii}	0.99	2.21(2)	3.08(2)	146

Symmetry codes for **1**: (i) 1/2 − *x*, −1/2 + *y*, 3/2 − *z*; (ii) −1/2 + *x*, 1/2 + *y*, *z*, (iii) −1/2 + *x*, −1/2 + *y*, *z*; **2**: (i) *x*, *y* + 1, *z*; (ii) *x*, *y*, *z* − 1; **3**: (i) 1 + *x* − *y*, *x*, 1/2 + *z*; (ii) 1 − *x* + *y*, *y*, 1/2 − *z*; (iii) 1 − *x* + *y*, 1 − *x*, *z*.

with a dihedral angle of 56.1(1), 66.7(1) and 78.8(1)°, respectively. The two hydrogenated imidazole five-member rings from each Bib ligand were not co-planar with the matrix benzene ring. Each Bib ligand in the binuclear cluster unit acted as a bidentate entity, two ligands acted in the *trans* configuration and the other ligand functioned in the *cis* mode, to ligate a pair of Co(II) ions by nitrogen atom from the five-member hydrogenated imidazole ring, which resulted in a triple-helical cluster structure (Fig. 1a and b and Scheme 2). Until now, there are a lot of triple helical metal–organic helicates have been reported. However, most of them are constructed by flexible ligands, such as bipyridine derivatives, terpyridine derivatives, 8-hydroxyquinoline derivatives *etc.*, and few examples are constructed by rigid ligands like Bib.[18]

The crystal packing of **1** exhibited an interesting feature in which the 1D chain, the 2D sheet and the well-shaped 3D layer network (Fig. 1c and d and ESI, Fig. S1),† which is quite common in organic supramolecular architectures[19] was stacked. The 1D chain (Fig. 1c) and the 2D supramolecular sheet (Fig 1d) are formed by N–H···Cl weak hydrogen bonds (Table 3) between the hydrogenated imidazole ring NH donors and Cl^- anion acceptors. Additionally, the C–H···Cl weak interactions and the N–H···H hydrogen bonds (Table 3) between the 2D sheets also found, which resulted in 3D supramolecular networks.

$[Co_2(Bib)_3Cl_2]Cl_2\cdot(CH_3OH)_2\cdot H_2O$, 2. The complex of **2** crystallized in the space group $P\bar{1}$, and the asymmetric unit contained two complex molecules. X-Ray single-crystal diffraction showed that the crystal structure of **2** consisted of discrete binuclear $[Co_2(Bib)_3Cl_2]^{2+}$ cations, one water molecule, two methanol molecules and two chloride anions. The binuclear $[Co_2(Bib)_3Cl_2]^{2+}$ cation, which was similar to **1**, is shown in Fig. 2a, and shows that the cation was also a triple-helical fashion. Each Co(II) ion was well coordinated to nitrogen atoms from three different ligands and a chloride anion, resulting in a highly distorted tetrahedral coordination geometry. The coordination angles around the Co(1) and Co(2) ions were in the range of 103.91(1)–115.4(2)° and 102.8(1)–118.9(2)°, respectively. In the binuclear cation, the Co–N and Co–Cl bond lengths were in the range of 1.998(4)–2.023(5) Å and 2.259(2)–2.264(2) Å, respectively, in which the Co–Cl bond length was also longer than that of the Co–N bond. These data are almost the same as those of **1**. The Co···Co separation in the cation was 5.584(2) Å, which was longer than that of **1**. It is worth noting that the Bib ligands acted in two ways in *cis* (C,A) and *trans* (A,A and C,C) coordination to the Co(II) ions with a *cis*–*trans* ratio of 1 : 2, as shown in Fig. 2a and Scheme 2. Three benzene rings from the Bib ligand in the $[Co_2(Bib)_3Cl_2]^{2+}$ cation were interlocked with each other at a dihedral angle of 51.6(1), 69.3(1), and 78.6(1)°, respectively. The two hydrogenated imidazole five-member rings from each Bib ligand were also not co-planar with the matrix benzene ring. Each Bib ligand in the binuclear cluster unit acted as a bidentate entity, two ligands acted in *trans* configuration and the other ligand functioned in *cis* mode, to ligate a pair of Co(II) ions by nitrogen atoms from the five-member hydrogenated imidazole ring, which resulted in a triple-helical cluster structure (Fig. 2a and b and Scheme 1). These results are similar to those of **1** apart from tiny differences. Nevertheless, it is interesting to note that there was a surprising structural feature of **1** and **2** in the solid structure. Although they had the same coordinated configurations, all Bib ligands adopted a different helical direction for **1** and **2**, respectively. (Fig. 1a and b and Fig. 2a and b).

The crystal packing of **2** exhibited a different feature (Fig. 2c and ESI, Fig. S2†) in which the 2D sheet and 3D structure, which were

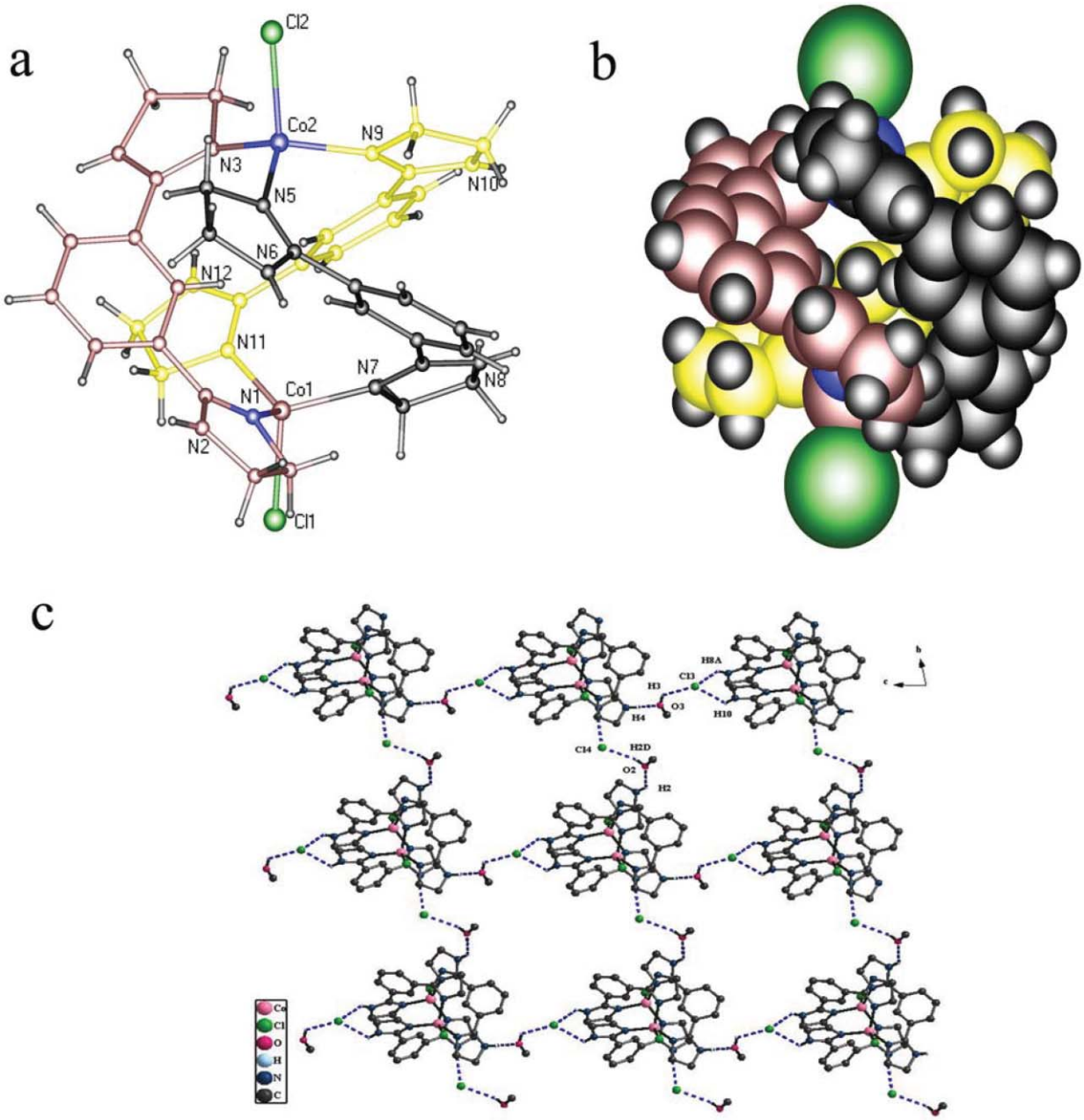

Fig. 2 (a) Perspective view of the binuclear cation in **2**. (b) Space-filling representation of the triple helical structure (c) 2D structure.

composed of binuclear $[Co_2(Bib)_3Cl_2]^{2+}$ cations was formed. The 2D sheet was caused by formation of O–H···Cl and N–H···Cl weak hydrogen bonds between the hydrogenated imidazole ring NH groups and the solvent water molecule OH groups donors and Cl^- anion acceptors (Table 3). It is worth noting that there were significant structural differences between **1** and **2** in the solid state. In **2**, there were more classic hydrogen bonds among chloride atoms from counter anions, oxygen atoms of methanol and water molecules and between nitrogen atoms from N–H groups of the hydrogenated imidazole ring (Table 3), which connected the 2D sheet into 3D supramolecular architecture. These findings may result in different magnetic and thermal properties between **1** and **2** in the solid state.

$[Co_3K_1(Tib)_2(CH_3COO)_6]PF_6$, 3. The complex **3** crystallizes in the hexagonal crystal system space group $P6_322$. The crystal structure of **3** featured $[Co_3K_1(Tib)_2(CH_3COO)_6]$ cluster cations and PF_6^- anions. As illustrated in Fig. 3a and c, the cluster cation possessed more fold axis passing through the center of ligand Tib. The K^+ cations and the P atom are localized on special positions: a three-fold axis passing through K^+ cations and P atom, which result in the occupancies of P, F1, F2 and F3 atoms with 0.16667, 0.5000, 0.16667 and 0.3333, respectively when the structure is refined. In addition, a 6_3 screw axis passes through the centroid of the phenyl ring in ligand Tib. In the $[Co_3K_1(Tib)_2(CH_3COO)_6]$ unit, each Co(II) ion was well coordinated to nitrogen atoms from two different ligands and two oxygen atoms from two acetate groups,

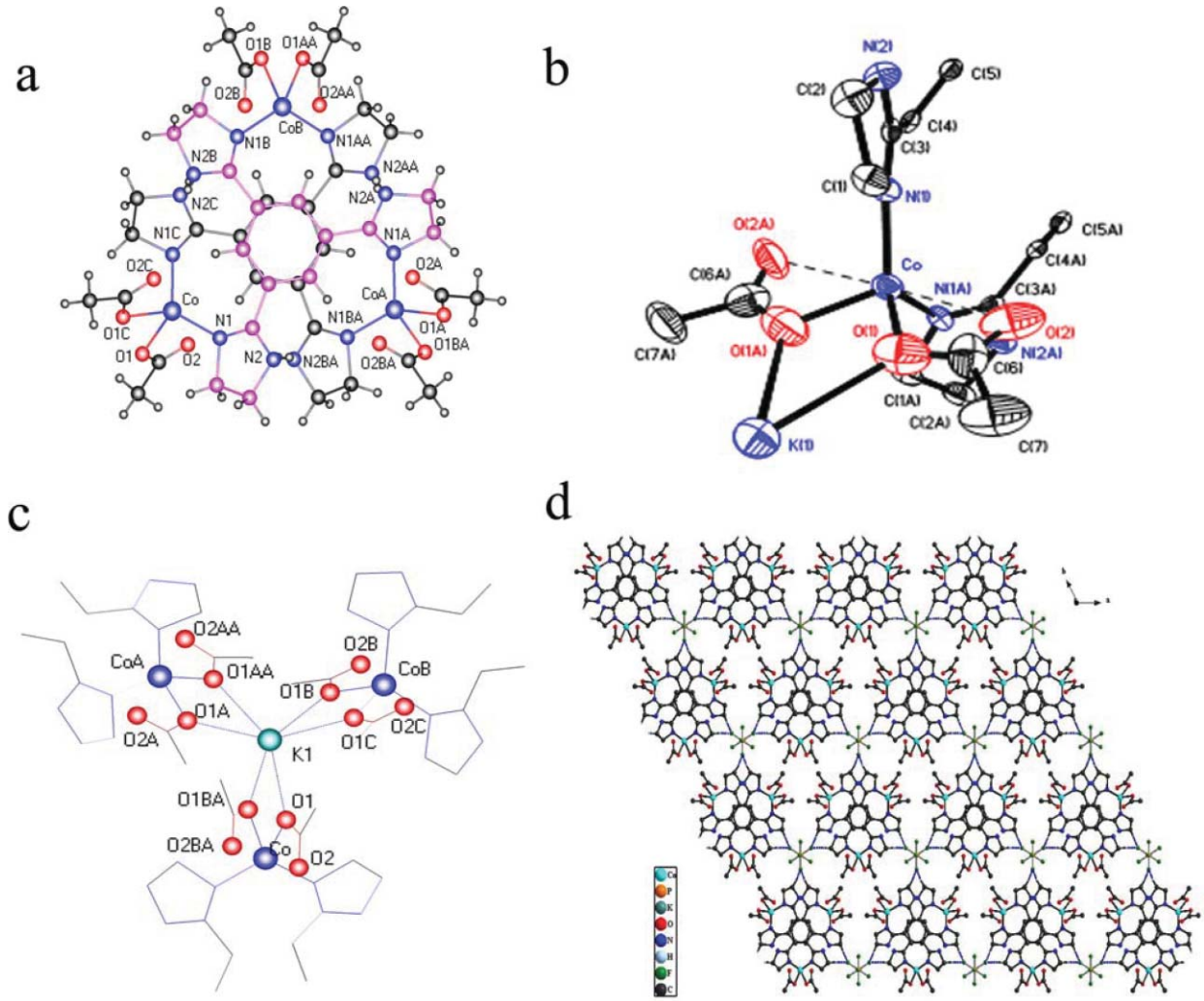

Fig. 3 (a) Perspective view of the trinuclear cation, (b) Co^{2+} coordination geometry, (c) K^+ coordination geometry, (d) packing of the 2D layers (no containing K^+).

resulting in a highly distorted tetrahedral coordination geometry (The distance of Co–O2 = 2.616(6) Å, it was obvious that there was no bond formation, due to weak contacts between Co ions and the O2 atom with two oxygen atoms. Further analysis demonstrated that O1, O1A, O2, O2A, Co and K1 atoms were all co-planar and the angles of ∠O2CoO2A and ∠O1CoO2 were 179.3(3) and 50.2(3)°, respectively, (Fig. 3b) which were not in agreement with the angle value of the octahedron. These data proved that the Co(II) ion was not in octahedral geometry). The bond angles around all the Co ions were in the range of 79.8 (6)–125.5(3)°, which deviated from the ideal value of 109.5°. In the cluster cation, the Co–N (2.026(5) Å) and Co–O (1.991(9) Å) bond lengths were almost equal. The three Co ions were at the apex of a triangle with a distance of 7.172 (1) Å and an angle of 60°. It is worth noting that the Tib ligands acted in an offset fashion in C,C,C and A,A,A coordination to the Co(II) ions, as shown in Fig. 3a and Scheme 1. Two benzene rings from the Tib ligand in the cluster cation were parallel to each other with a face-to-face distance of 3.315(1) Å, indicating that there was a strong π–π stacking interaction between the pair of benzene rings. The three hydrogenated imidazole five-member rings from each Tib ligand were not co-planar with the matrix benzene ring. Each Tib ligand in the cluster unit acted as a tridentate entity to ligate three Co(II) ions by nitrogen atom from the five-member hydrogenated imidazole ring, which resulted in a cylinder-like cluster structure.

The crystal packing of **3** exhibited the well-shaped 2D honeycomb layer network (Fig. 3d), which is quite common in organic supramolecular architectures.[19] Such stacking of the 2D layers is caused by formation of C–H···F weak hydrogen bonds between the hydrogenated imidazole ring CH donors and the F atom of PF_6^- group acceptors (Fig. 3d and Fig. 3b). The basic unit of the honeycomb network was composed of three cluster $[Co_3(Tib)_2]$ cations three PF_6^- groups, a K^+ cations and three CH_3COO groups due to six non-classic weak hydrogen bonds (C–H···F) (Fig. 3d and ESI, Fig. S3b).† It was noted in the packing of **3** (ESI, Fig. S3a and S3c†) that there were more no-classic hydrogen bonds C–H···O hydrogen bonds and N–H···O classic hydrogen bonds (Table 3) between the adjacent 2D layer, which connected the 2D layers into a 3D supramolecular architecture (ESI, Fig. S3a and S3c).†

Magnetic properties

{[Co_2(Bib)$_3$$Cl_2$]Cl(CH$_3$COO)}·CH$_3$OH·$H_2O$, 1. The temperature-dependent magnetic susceptibilities of compound **1** were investigated at a temperature range of 2–300 K, in the form of χ_M and $\chi_M T$ *vs.* T, and are represented in Fig. 4, respectively, where χ_M is the molar susceptibility for **1**. The susceptibility data between 100–300 K followed the Curie–Weiss law with a Weiss constant $\theta = -12.3$ K and a Curie constant of $C = 5.31$ emu K mo1^{-1}, indicating that there was an antiferromagnetic interaction between two adjacent cobalt(II) ions. The $\chi_M T$ value per Co_2 unit (5.15 emu K mol^{-1}) at room-temperature is much higher than the expected spin-only value for $S = 3/2$ (3.75 emu K mol^{-1}) in tetrahedral geometry. Upon cooling the sample, $\chi_M T$ basically stays from 5.15 to 4.74 emu K mol^{-1} in the range of 300–60 K, then show an abrupt increase to a maximum value of 27.94 emu K mol^{-1} at 14 K. Below this temperature, the $\chi_M T$ drops rapidly to a value of 6.64 emu K mol^{-1} at 2 K. Taking into account the dimmer character in the structure of compound **1**, the $\chi_M T$ data were fitted by using the isotropic Heisenberg model $\hat{H} = -2J\hat{S}_A\hat{S}_B$ for two interacting $S = 3/2$ centers to determine the exchanging parameters *via* the Bib ligands.[20]

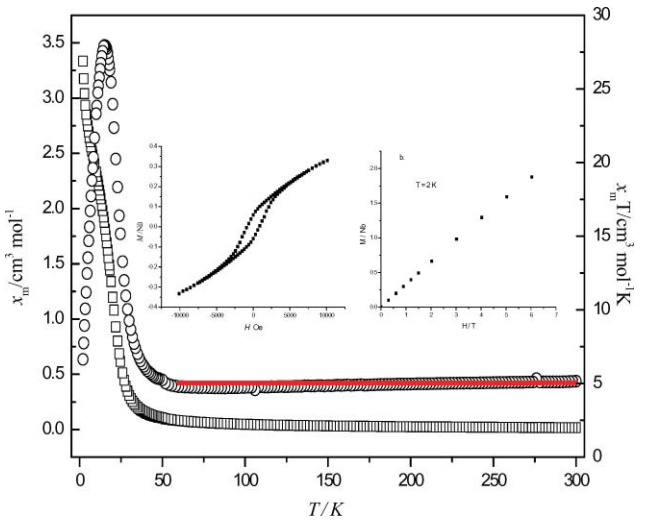

Fig. 4 Plot of χ_M (block) and $\chi_M T$ *vs.* T (blue) in the 340–2 K range of temperatures for **1** measured under external magnetic field of 0.1 T, respectively. Inset: (a) hysteresis loop, (b) M–H curve at 2 K.

$$\chi_m T = \frac{2Ng^2\beta^2}{k}\frac{e^{-2x} + 5e^{-6x} + 14e^{-12x}}{1 + 3e^{-2x} + 5e^{-6x} + 7e^{-12x}} \quad (1)$$

$$x = -J/kT \quad (2)$$

The best fit for calculated and experimental data was achieves above 60 K for $J = -2.07$ cm^{-1} and $g = 2.35$ with the agreement factor $R = \Sigma(\chi_m T_{exp} - \chi_m T_{cal})^2/\Sigma(\chi_m T_{exp})^2$ of 3.4×10^{-5}.

Below 15 K the $\chi_m T$ product experiences an upturn, reaching 27.94 emu K mol^{-1} at 14 K with an applied field of 500 Oe. This low temperature behaviour suggests the occurrence of ferromagnetic ordering in **1**, which may arise from the presence of canting between the antiparallel alignment of the spins.[21] The hysteresis loop measured at 2 K shows values of the coercive field (H_C) and remnant magnetization (M_R) of 881 Oe and 0.038 $N\beta$ mol^{-1}, respectively, being characteristic of a soft magnet. It is well known that the occurrence of spin canting is usually caused by either single-ion magnetic anisotropy or antisymmetric exchange in magnetic entities. Because there is not an inversion center in the Co_2 entity and Co^{2+} ions has large magnetic anisotropy, the observation of the spin canting in **1** should arise from the antisymmetric exchange in the dinuclear entity together with the anisotropy of the Co^{2+} ions.[22]

To obtain the critical temperature of the long-range magnetic ordering precisely, the ac magnetic susceptibility measurements were performed under $H_{ac} = 1000$ Oe and a frequency range of 1–397 Hz. Surprisingly, both the in-phase and out-of-phase signals, χ_M' and χ_M'', display a maximum which is frequency dependent (Fig. 5), implying a slow relaxation process. This slow relaxation process could be caused by either domain wall movements[23] or spin-glass behaviours.[24] The shift of the peak temperature (T_p) of χ_M' is measured by a parameter $\phi = (\Delta Tp/Tp)/\Delta(\log f) = 0.03$ (f is the frequency of H_{ac}), which is in the range of a normal spin-glass. The frequency dependence of T_p on χ_M'' can be fitted well to the Arrhenius law: $\tau(T) = \tau_0 \exp(\Delta/k_B T)$, where τ_0 is the pre-exponential factor and Δ is the energy gap. The best fit results in parameters $\tau_0 = 1.2 \times 10^{-10}$ s and $\Delta/k_B = 46$ K. The activation energy may be compared with those typical for the domain wall movements.[23]

[Co_2(Bib)$_3$$Cl_2$]$Cl_2$(CH$_3$OH)$_2$$H_2O$, 2. The temperature-dependent magnetic susceptibilities of compound **2** were investigated in the temperature range of 2–300 K, in the form of χ_M and $\chi_M T$ *vs.* T, are represented in Fig. 6, respectively,

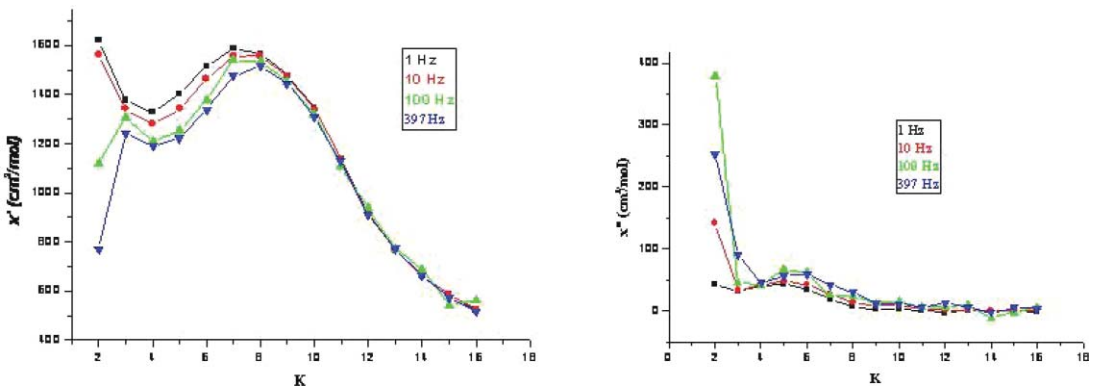

Fig. 5 Temperature dependence of zero-field ac magnetic susceptibility for **1**.

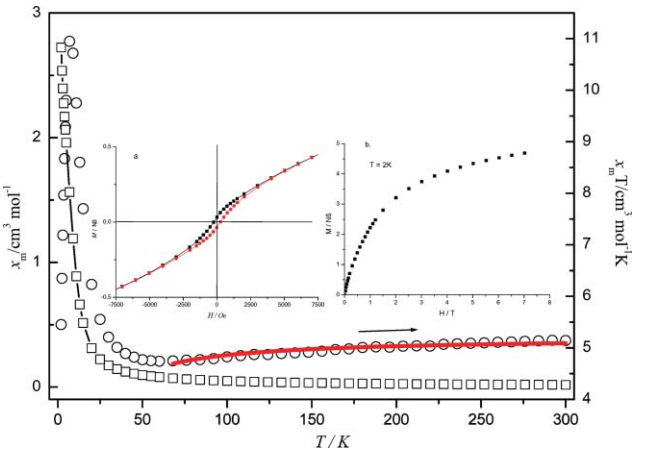

Fig. 6 Plot of χ_M (block) and $\chi_M T$ *vs.* T (blue) in the 300–2 K range of temperatures for **2** measured under external magnetic field of 0.1 T, respectively. Inset: (a) hysteresis loop, (b) M–H curve at 2 K.

where χ_M is the molar paramagnetic susceptibility for **2**. The susceptibility data between 70–300 K follows the Curie–Weiss law with a Weiss constant $\theta = -9.8$ K and Curie constant of $C = 5.32$ emu K mol^{-1}, indicating that there is an antiferromagnetic interaction between neighbouring cobalt(II) ions. $\chi_M T$ value per Co_2 unit (5.14 emu K mol^{-1}) at room-temperature is much higher than the expected spin-only value for $S = 3/2$ (3.75 emu K mol^{-1}) in tetrahedral geometry. Upon cooling the sample, $\chi_M T$ decrease slowly from 5.14 to 4.74 emu K mol^{-1} in the range of 300–70 K, then shows an abrupt increase to a maximum value of 11.0 emu K mol^{-1} at 6.7 K. Below this temperature, the $\chi_M T$ drops rapidly to a value of 5.45 emu K mol^{-1} at 2 K. To determine the exchange parameters *via* three bib ligands, $\chi_m T$ was fitted by using a dimmer isotropic Heisenberg model $\hat{H} = -2J\hat{S}_1\hat{S}_2$ for two interacting $S = 3/2$ centers as well as compound **1**. The best fit for calculated and experimental data was achieved above 70 K for $J = -1.83$ cm^{-1} and $g = 2.36$ with the agreement factor $R = \Sigma(\chi_m T_{exp} - \chi_m T_{cal})^2/\Sigma(\chi_m T_{exp})^2$ of 3.7×10^{-5}. The coupling interactions in the two dimmers are of same magnitude, which is consistent with the similar structures in compound **1** and **2**.

Below 50 K an abrupt increase in $\chi_M T$ *vs.* T was observed, suggesting a ferromagnetic phase transition.[25] This low temperature behaviour may arise from the presence of canting between the antiparallel alignment of the spins[26]. Furthermore, a hysteresis loop was observed at 2 K with a coercive field (H_C) of 265 Oe and remnant magnetization (M_R) of 0.032 $N\beta$ mol^{-1} (Fig. 6, Inset a), indicating a soft-magnet-type behaviour. The data from an M–H curve at 2 K (Fig. 6, Inset b) showed that the magnetization attained a highest value at 7 KOe. As well as **2**, the observation of the spin canting in **2** should arise from the antisymmetric exchange in the dinuclear entity together with the anisotropy of the Co^{2+} ions because they have similar molecular structures.[22]

The zero-field ac magnetic susceptibility measurements were performed under 1–997 Hz. Surprisingly, both the in-phase and out-of-phase signals, χ_M' and χ_M'', display a maximum which is strong frequency dependent (Fig. 7), implying a slow relaxation process. This slow relaxation process could be caused by either domain wall movements[23] or spin-glass behaviours.[24] The shift of the peak temperature (T_p) of χ_M' is measured by a parameter $\phi = (\Delta T_p/T_p)/\Delta(\log f) = 0.01$ (f is the frequency of H_{ac}), which

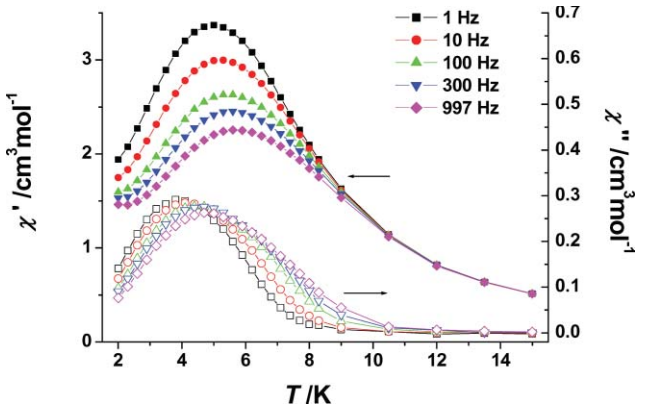

Fig. 7 Temperature dependence of zero-field ac magnetic susceptibility for **1**.

is in the range of a normal spin-glass. The relaxation time τ may be calculated from the Arrhenius law, leading to parameters frequency $\tau_0 = 2.1 \times 10^{-17}$ s and $\Delta/k_B = 131$ K. The activation energy may be compared with those typical for the domain wall movements,[23] although the τ_0 value is too small.

The observation of canted antiferromagnetism in **1** and **2** is not unexpected due to the unsymmetrical exchange couplings between the neighbouring metal ions. However, the coexistence of the slow relaxation process is unusual. This relaxation process could be due to the spin-glass behaviours and/or domain wall movements. The small ϕ values obtained from the frequency dependence of T_p on χ_M' support a spin-glass behaviour in **1** and **2**, while the activation energies obtained from the frequency dependence of T_p on χ_M'' suggest the presence of domain wall movements. Apparently, **1** and **2** showed quite unusual magnetic behaviours and were tentatively ascribed to the canted antiferromagnetism with spin-glass-like relaxation. Since the randomness (defects, disorder, *etc.*) and frustration (geometrical or competitive) are responsible for the spin-glass system[21], the spin-glass-like behaviour of **1** and **2** could be related to possible crystal defects and/or the presence of some degree of superparamagnetic relaxation of the magnetization of **1** and **2**.

Conclusion

In this work we have synthesized and characterized three novel coordinated compounds $\{[Co_2(Bib)_3Cl_2]Cl(CH_3COO)\}\cdot CH_3OH\cdot H_2O$, (**1**), $[Co_2(Bib)_3Cl_2]Cl_2\cdot(CH_3OH)_2\cdot H_2O$, (**2**) and $[Co_3K_1(Tib)_2(CH_3COO)_6]PF_6$ (**3**) (Bib = 1,3-bis(4,5-dihydro-1*H*-imidazol-2-yl)benzene; Tib = 1,3,5-tris(4,5-dihydro-1*H*-imidazol-2-yl)benzene). In the crystal structure of binuclear triple-helical $[Co_2(Bib)_3Cl_2]^{2+}$ cations in **1** and **2**, each Co(II) ion was in a highly distorted tetrahedral coordination geometry with a *cis–trans* ratio of 1 : 2 from the Bib ligand. In the $[Co_3K_1(Tib)_2(CH_3COO)_6]$ unit in **3**, each Co(II) ion was also in a highly distorted tetrahedral coordination geometry and the Tib ligands acted in an offset fashion in C,C,C and A,A,A coordination to the Co(II) ions with π–π stacking interactions between two benzene rings from the Tib ligand in the cluster cation. Each Tib ligand in the cluster unit acted as a tridentate entity to ligate three Co(II) ions resulting in a cylinder-like cluster structure. The intermolecular hydrogen bonds in the solid-state resulted in the well-shaped 2D

layer network which was formed in a honeycomb hexagonal ring and 3D supramolecular architecture in **1**, the 3D supramolecular architecture which was connected to the 2D sheet into 3D for **2** and the 3D supramolecular architecture which was extended to a well-shaped 2D sheet layer network for **3**. The results from magnetic data, in the high-temperature region, showed that **1** and **2** obeyed the Curie–Weiss law with an antiferromagnetic interaction property. In addition, **1** and **2** showed magnetic ordering at low temperature due to the canting effect. The zero-field ac magnetic susceptibility measurements for **1** and **2** displayed a maximum, which was frequency dependent owing to a slow relaxation process, which could be caused by either domain wall movements or spin-glass behaviours.

Acknowledgements

This work was financially supported by LADPSHNU (DZL806), NSFC (50802059), FSHE (07ZZ68), KSTS (065212050), SLADP (S30406), KLSH (07dz22303), SMEC (08YZ68) and SNU (PL619 and SK200718).

References

1 P. J. Steel, *Acc. Chem. Res.*, 2005, **38**, 243.
2 B. Moulton and M. J. Zaworotko, *Chem. Rev.*, 2001, **101**, 1629.
3 (*a*) P. Gamez and J. Reedijk, *Eur. J. Inorg. Chem.*, 2006, **24**, 29; (*b*) A. N. Khlobystov, A. J. Blake, N. R. Champness, D. A. Lemenovskii, A. G. Majouga, N. V. Zyk and M. Schroder, *Coord. Chem. Rev.*, 2001, **222**, 155.
4 (*a*) M. Murrie, S. J. Teat, H. Stoeckli-Evans and H. U. Güdel, *Angew. Chem., Int. Ed.*, 2003, **42**, 4653; (*b*) X. Y. Wang, L. Wang, Z. M. Wang and S. Gao, *J. Am. Chem. Soc.*, 2006, **128**, 674; (*c*) S. M. Humphrey and P. T. Wood, *J. Am. Chem. Soc.*, 2004, **126**, 13236; (*d*) H. Nakamura, Y. Sunatsuki, M. Kojima and N. Matsumoto, *Inorg. Chem.*, 2007, **46**, 8170; (*e*) X. J. Li, X. Y. Wang, S. Gao and R. Cao, *Inorg. Chem.*, 2006, **45**, 1508; (*f*) M. H. Zeng, M. X. Yao, H. Liang, W. X. Zhang and X. M. Chen, *Angew. Chem., Int. Ed.*, 2007, **46**, 1; (*g*) G. J. T. Cooper, G. N. Newton, P. Kögerler, D. L. Long, L. Engelhardt, M. Luban and L. Cronin, *Angew. Chem., Int. Ed.*, 2007, **46**, 1340; (*h*) Y. Z. Zheng, M. L. Tong, W. X. Zhang and X. M. Chen, *Angew. Chem., Int. Ed.*, 2006, **45**, 6310; (*i*) A. K. Boudalis, C. P. Raptopoulou, B. Abarca, R. Ballesteros, M. Chadlaoui, J. P. Tuchagues and A. Terzis, *Angew. Chem., Int. Ed.*, 2006, **45**, 432.
5 (*a*) B. L. Chen, C. D. Liang, J. Yang, D. S. Contreras, Y. L. Clancy, E. B. Lobkovsky, O. M. Yaghi and S. Dai, *Angew. Chem., Int. Ed.*, 2006, **45**, 1390; (*b*) G. J. Halder, C. J. Kepert, B. Moubaraki, K. S. Murray and J. D. Cashion, *Science*, 2002, **298**, 1762; (*c*) C. D. Wu, A. Hu, L. Zhang and W. B. Lin, *J. Am. Chem. Soc.*, 2005, **127**, 8940; (*d*) P. Day and A. E. Underhill, *Metal–Organic and Organic Molecular*, The Royal Society, 1999; (*e*) W. Fujita, K. Awaga, R. Kondo and S. Kagoshima, *J. Am. Chem. Soc.*, 2006, **128**, 6016; (*f*) M. Murugesu, W. Wernsdorfer, K. A. Abboud and G. Christou, *Angew. Chem., Int. Ed*, 2005, **44**, 892; (*g*) E. E. Moushi, T. C. Stamatatos, W. Wernsdorfer, V. Nastopulos, G. Christou and A. J. Tasiopoulos, *Angew. Chem., Int. Ed*, 2006, **45**, 7722.
6 (*a*) J. S. Miller and M. Drilon, *Magnetism, Molecules to Materials (I–IV)*, Willey-VCH, Weinheim, 2002; (*b*) D. B. Zhu, *Advances in Function Materials*, Chemical Industry Press, 2005; (*c*) E. Coronao, F. Palacio and J. Veciana, *Angew Chem., Int. Ed.*, 2003, **42**, 2570; (*d*) T. C. Stamataos, K. A. Abboud, W. Wernsdorfer and G. Christou, *Angew. Chem., Int. Ed*, 2007, **46**, 884; (*e*) C. M. Zaleski, E. C. Depperman, C. Dendrinou-Samara, M. Alexiou, J. W. Kampf, D. P. Kessissoglou, M. L. Kirk and V. L. Pecoraro, *J. Am. Chem. Soc.*, 2005, **127**, 12862; (*f*) L. Lecren, W. Wernsdorfer, Y. G. Li, O. Roubeau, H. Miyasaka and R. Clerac, *J. Am. Chem. Soc.*, 2005, **127**, 11311; (*g*) E. Coronado, A. Forment-Aliaga, A. Gaita-Arino, F. M. Romero and W. Wernsdorfer, *Angew. Chem., Int. Ed*, 2004, **43**, 6152.
7 (*a*) S. Maheswaran, G. Chastanet, S. J. Teat, R. Sessoli, W. Wernsdorfer and R. E. P. Winpenny, *Angew. Chem., Int. Ed*, 2005, **44**, 5044; (*b*) A. M. AKo, I. J. Hewitt, V. Mereacre, R. Clerac, W. Wersdorfer, C. E. Anson and A. K. Powell, *Angew. Chem., Int. Ed*, 2006, **45**, 4926; (*c*) Y. L. Bai, J. Tao, W. Wernsdorfer, O. Stato, R. B. Huang and L. S. Zheng, *J. Am. Chem. Soc.*, 2006, **128**, 16428; (*d*) C. Yang, W. Wernsdorfer, G. H. Lee and H. L. Tsai, *J. Am. Chem. Soc.*, 2007, **129**, 456; (*e*) H. Oshio, N. Hoshino, T. Ito and M. Nakano, *J. Am. Chem. Soc.*, 2004, **126**, 8805; (*f*) A. Cornia, A. C. Fabretti, P. Garrisi, C. Mortalo, D. Bonacchi, D. Gatteschi, R. Sessoli, L. Sorace, W. Wernsdorfer and A. L. Barra, *Angew. Chem., Int. Ed*, 2004, **43**, 1136.
8 (*a*) G. W. Powell, H. N. Lancashire, E. K. Brechin, D. Collison, S. L. Heath, T. Mallah and W. Wersdorfer, *Angew. Chem., Int. Ed*, 2004, **43**, 5772; (*b*) T. F. Liu, D. Fu, S. Gao, Y. Z. Zhang, H. L. Sun, G. Su and Y. J. Liu, *J. Am. Chem. Soc.*, 2003, **125**, 13976; (*c*) Y. Z. Zhang, W. Wernsdorfer and S. Gao, *Chem. Commun.*, 2006, 3302; (*d*) S. C. Xiang, X. T. Wu, J. J. Zhang, R. B. Fu, S. M. Hu and X. D. Zhang, *J. Am. Chem. Soc.*, 2005, **127**, 16352; (*e*) S. Accors, A. L. Barra, A. Caneschi, G. Chastanet, A. Cornia, A. C. Fabretti, D. Gatteschi, C. Mortalo, E. Olivier, F. Parenti, P. Rosa, R. Sessoli, L. Sorace, W. Wernsdorfer and L. Zobbi, *J. Am. Chem. Soc.*, 2006, **128**, 4742.
9 (*a*) H. Miyasaka, R. Clerac, W. Wernsdorfer, L. Lecren, C. Bonhomme, K. I. Sugiura and M. Yamashita, *Angew. Chem., Int. Ed*, 2004, **43**, 2801; (*b*) M. Ferbinteanu, H. Miyasaka, W. Wernsdorfer, K. Nakata, K. I. Sugiura, M. Yamashita, C. Claude and R. Clerac, *J. Am. Chem. Soc.*, 2005, **127**, 3090; (*c*) D. F. Li, S. Parkin, G. B. Wang, G. T. Yee, R. Clerac, W. Wernsdorfer and S. M. Holmes, *J. Am. Chem. Soc.*, 2006, **128**, 4214; (*d*) Y. Song, P. Zhang, X. M. Ren, X. F. Shen, Y. Z. Li and X. Z. You, *J. Am. Chem. Soc.*, 2005, **127**, 3708; (*e*) J. K. Lim, J. H. Yoon, H. C. Kim and C. S. Hong, *Angew. Chem., Int. Ed*, 2006, **45**, 7424; (*f*) W. G. Wang, A. J. Zhou, W. X. Zhang, M. L. Tong, X. M. Chen, M. Nakano, C. C. Beedle and D. N. Hendrickson, *J. Am. Chem. Soc.*, 2007, **129**, 1014.
10 (*a*) S. P. Yang, X. M. Chen and L. N. Ji, *J. Chem. Soc., Dalton Trans.*, 2000, 2337; (*b*) L. S. Long, S. P. Yang, T. X. Tong, Z. W. Mao, X. M. Chen and L. N. Ji, *J. Chem. Soc., Dalton Trans.*, 1999, 1999; (*c*) S. P. Yang, L. S. Long, X. M. Chen and L. N. Ji, *Acta Crystallogr., Sect. C: Cryst. Struct. Commun.*, 1999, **55**, 869; (*d*) S. P. Yang, H. L. Zhu, X. M. Chen and L. N. Ji, *Polyhedron*, 2000, **19**, 2237; (*e*) S. P. Yang, Y. X. Tong, H. L. Zhu, H. Cao, X. M. Chen and L. N. Ji, *Polyhedron*, 2001, **20**, 223.
11 (*a*) H. M. Chen, S. P. Yang, F. Zhang and X. B. Yu, *Synth. React. Inorg. Met.-Org. Chem.*, 2003, **33**, 1787; (*b*) S. P. Yang, H. M. Chen, F. Zhang and X. B. Yu, *Appl. Organomet. Chem.*, 2004, **18**, 88; (*c*) S. P. Yang, H. M. Chen, F. Zhang, Q. Q. Chen and X. B. Yu, *Acta Crystallogr., Sect. E: Struct. Rep. Online*, 2004, **60**, m465; (*d*) H. M. Chen, S. P. Yang, F. Zhang, Q. Q. Chen and X. B. Yu, *Acta Crystallogr., Sect. E: Struct. Rep. Online*, 2005, **61**, m1001 and m1277; (*e*) J. J. Sun and S. P. Yang, *Acta Crystallogr., Sect. E: Struct. Rep. Online*, 2006, **62**, m3144.
12 C. X. Ren, B. H. Ye, F. He, L. Cheng and X. M. Chen, *CrystEngComm*, 2004, **6**, 200–206.
13 (*a*) A. Kraft and F. Osterod, *J. Chem. Soc., Perkin Trans. 1*, 1998, **6**, 1019; (*b*) A. Kraft and A. Reichert, *Tetrahedron*, 1999, **55**, 3923; (*c*) A. Kraft and R. Fröhlich, *Chem. Commun.*, 1998, **10**, 1085.
14 C. J. O'Connor, *J. Prog. Inorg. Chem.*, 1982, **29**, 203.
15 R. Blessing, *Acta Crystallogr. Sect. A: Found. Crystallogr.*, 1995, **51**, 33.
16 (*a*) G. M. Sheldrick, *SHELXS-97, Program for solution of crystal structures*, University of Göttingen, Germany, 1997; (*b*) G. M. Sheldrick, *SHELXL-97, Program for refinement of crystal structures*, University of Göttingen, Germany, 1997.
17 *International Tables for X-Ray Crystallography*, vol. C, Tables 4.2.6.8 and 6.1.1.4. Kluwer Academic Publisher, Dordrecht, 1992.
18 (*a*) L. J. Charbonnière, A. F. Williams, C. Piguet, G. Bernardinelli and E. Rivara-Minten, *Chem.–Eur. J.*, 1998, **4**, 485; (*b*) G. S. Subramanya and P. Samudranil, *Inorg. Chem.*, 2005, **44**, 6299; (*c*) C. Paula, P. Mirela, S. Roberta, A. Narcis, Avarvari, P. Fabrice and A. Marius, *Inorg. Chem.*, 2006, **45**, 7035; (*d*) D. Guo, K. L. Pang, C. Y. Duan, C. He and Q. J. Meng, *Inorg. Chem*, 2002, **41**, 5978; (*e*) C. Piguet, G. Bernardinelli, B. Bocquet, A. Quattropani and A. F. Williams, *J. Am. Chem. Soc.*, 1992, **114**, 7440; (*f*) M. Albrecht, *Chem. Rev.*, 2001, **101**, 3457; (*g*) C. Piguet, M. Borkovec, J. Hamacek and K. Zeckert, *Coord. Chem. Rev.*, 2005, **249**, 705.
19 (*a*) B. Moulton and M. J. Zaworotko, *Chem. Rev.*, 2001, **101**, 1629; (*b*) F. H. Herbstein, M. Kapon and G. M. Reisner, *J. Inclusion Phenom.*, 1987, **5**, 211; (*c*) F. H. Herbstein, *Top. Curr. Chem.*, 1987, **140**, 107; (*d*) K. Biradha, D. Dennis, V. A. MacKinnon, C. V. K. Sharma and

M. J. Zaorotko, *J. Am. Chem. Soc.*, 1988, **120**, 11894; (*e*) J. J. Jiang, X. P. Li, X. L. Zhang, B. S. Kang and C. Y. Su, *CrystEngComm*, 2005, **7**, 603.
20 T. Ishida, T. Kawakami, S.-i. Mitsubori, T. Nogami, K. Yamaguchi and H. Iwamura, *J. Chem. Soc., Dalton Trans.*, 2002, 3177.
21 (*a*) D. Armentano, G. De, Munno, T. F. Mastropietro, M. Julve and F. Lloret, *J. Am. Chem. Soc.*, 2005, **127**, 10778; (*b*) D. Armentano, G. De, Munno, T. F. Mastropietro, D. M. Proserpio, M. Julve and F. Lloret, *Inorg. Chem.*, 2004, **43**, 5177; (*c*) A. K. Boudalis, C. P. Raptopoulou, B. Abarca, R. Ballesteros, M. Chadlaoui, J.-P. Tuchagues and A. Terzis, *Angew. Chem., Int. Ed*, 2006, **45**, 432.
22 L. A. Barrios, J. Ribas, G. Aromí, J. Ribas-Ariño, P. Gamez, O. Roubeau and S. J. Teat, *Inorg. Chem.*, 2007, **46**, 7154.
23 (*a*) F. Bellouard, M. Clemente-León, E. Coronado, J. R. Galán-Mascarós, C. J. Gómez-García, F. Romero and K. P. Dunbar, *Eur. J. Inorg. Chem.*, 2002, **20**, 1603; (*b*) E. Coronado, C. J. Gómez-García, A. Nuez, F. M. Romero, E. Rusanov and H. Stoeckli-Evans, *Inorg. Chem.*, 2002, **41**, 4615; (*c*) D. K. Cao, Y. Z. Li and L. M. Zheng, *Inorg. Chem.*, 2007, **46**, 7571.
24 J. A. Mydosh, *Spin Glasses: An Experimental Introduction*, Taylor & Francis, London, 1993.
25 S. C. Xiang, X. T. Wu, J. J. Zhang, R. B. Fu, S. M. Hu and X. D. Zhang, *J. Am. Chem. Soc.*, **127**, 16353.